SURFACE INTEGRITY AND TRIBOLOGICAL BEHAVIOR OF PLASMA SPRAYED ALUMINA COATINGS ON STEEL AND ALUMINUM SUBSTRATES

N.M. Vaxevanidis[1], D.E. Manolakos[2] and G.P. Petropoulos[3]
[1] Hellenic Air-Force Academy, Dekelia Air-Force Base, Attica, Greece
[2] Manufacturing Technology Division, National Technical University of Athens, Athens, Greece
[3] Department of Mechanical and Industrial Engineering, University of Thessaly, Volos, Greece

Abstract

Ceramic coatings produced by thermal spray techniques are widely used to improve wear and corrosion resistance of working metal surfaces. In the present paper we report on the surface integrity states and the tribological behaviour of plasma-sprayed alumina coatings on steel and aluminum substrates. The influence of arc current employed during the spraying processes on the two previous mentioned aspects is also examined.

Keywords*: tribology testing, plasma spraying, surface integrity, wear mechanisms.*

1. INTRODUCTION

Nowadays it has been realized that the surface is the most important part of any engineering component. It is from surface-initiated effects that most components fail. Technological advance is often constrained by surface demands. In a great number of applications, mechanical components operate under severe conditions; therefore a type of surface modification is necessary in order to enhance functional integrity and/or avoid possible failure or degradation. The term 'surface engineering' encompasses all those techniques and processes which are used in order to modify and enhance the performance of an engineering surface. This term usually covers three major categories of interrelated activities [1]: (i) optimization of surface properties, (ii) coatings technology and (iii) characterization of coatings.

Ceramic coatings produced by thermal spray techniques are widely used for a range of industrial applications as thermal barriers and/or abrasion, erosion or corrosion resistant coatings. The aerospace industry is a large consumer of thermal barrier coatings as well as of abrasion and erosion resistant coatings. Note also that

thermal barrier coatings have also made their entrance into the area of combustion engines [2]. Alumina coatings, are commonly used to resist wear by solid particle erosion and friction due to their high hardness and chemical stability even at elevated temperatures [3, 4]. The use of ceramic coatings in tribological applications is now well documented [5] and it is not discussed here. From a practical point of view, plasma spraying is a rather simple process. By means of a plasma the coating material is heated to a molten or plastic state and rapidly propelled in the form of droplets or soft particles towards the substrate where they spread out and solidify to produce a covering protective coating. The plasma is produced by means of an electric discharge in either a clean gas or in a mixture of several gases. Frequently used gases are argon, nitrogen and hydrogen. Plasma spraying is widely used to produce thick (100 - 300 μm), high density ceramic coatings on a range of components. The technique produces some unique microstructural features which have a considerable influence on the physical properties of the coatings; the morphology of the splats, the amount of intersplat bonding and the level of

porosity within the coating exert a major influence on its strength and adhesion to the substrate. It is thus likely that the structure of the coating will have an important effect on its wear performance [6].

The structure of the coating is a function of the melting of ceramic particles in the plasma and their impact velocity which are controlled by the choice of processing conditions. In general, poor particle melting and low velocity at impact lead to high levels of porosity and poor intersplat bonding, as the case in air plasma spraying (APS). However, the use of a low pressure inert environment (typically 100 mbar argon) in so-called low pressure or vacuum plasma spraying (VPS) significantly improves coating density and intersplat bonding [6].

Plasma spraying and similar techniques are now well established as "surface modification" commercial processes; see [7] and the review of relevant advances is beyond the scope of this paper. The present paper is focused on the study of the surface integrity states and the tribological behavior of plasma-sprayed alumina coatings on steel (Ck 45) and aluminum (O-T3) substrates. The influence of arc current employed during the spraying processes on the two previous mentioned aspects is also examined.

2. EXPERIMENTAL

2.1 Plasma spraying

The substrates to be coated were made of Ck 45 tool steel and aluminum alloy 2030-O-T3 in the form of discs with diameter d = 50 mm and thickness t = 6 mm. Prior to deposition, specimens were sandblasted, in order to increase their surface roughness and achieve better adherence between the ceramic coating and the metallic substrate. For the same purpose, an intermediate bond layer of 80 wt. % Ni – 20 wt. % Al was applied on the surface to be coated, by the same APS technique. The alumina coating as well as the bond layer were realized in a number of successive passes. For the deposition of the bond and the upper layer a Miller SG 100 - Thermal Atmospheric Plasma Spraying equipment with Motoman Robotec robotic arm was used. The characteristics of the powders and the spraying conditions are summarized in Table 1.

Table 1: Powders characteristics and spraying conditions for the deposition of the metallic bond and the ceramic upper layer

	Bond layer (Ni–20% Al)	Ceramic layer (Al_2O_3)
Powder characteristics		
Type	Metco 404	Metco 101
Grain size	-100+30	-45+%
Operating conditions		
Arc current (A)	700- 800	variable
Arc voltage (V)	38-40	65
Primary plasma gas	Ar	Ar
Pressure (MPa)	0.35	0.35
Secondary plasma gas	He	He
Pressure (MPa)	0.75	0.68
Feeding gas	Ar	Ar
Powder feed rate (g/m)	40	25
Spraying distance (mm)	100	82
Number of passes	19 (22)	46 (48)

Numbers in brackets refer to aluminium substrate.

During spraying of the ceramic coating the operating parameters were kept constant, with only the arc current varying (I = 500, 550 and 600 A) resulting in six different specimen types designated X1, X2, X3 (for steel substrate) and A1, A2 and A3 (for aluminum alloy substrate).

2.2 Surface integrity evaluation

The as-sprayed coatings, before the subsequent tribological testing, were evaluated in terms of surface integrity [8] by using standard metallographic methods, microhardness testing and surface profilometry.

The microstructure of the coated samples were observed under a metallographic microscope (Leica DMR) with image analysis software (Image Pro) whilst microhardness testing was performed on a Shimadzou HVM-200 tester equipped with a Vickers indenter under a load of 5 N; the microhardness values obtained being

the average of five indentations.

Surface roughness was measured with a Rank Taylor-Hobson Surtronic 3+ profilometer equipped with the Talyprof software. The cut-off length was selected at 0.8 mm whilst 10 measurements were conducted on each specimen.

2.3 Tribological testing

For the evaluation of friction and wear characteristics sliding friction tests were performed on a state-of-the-art CSEM pin-on-disc apparatus properly modified to accommodate pins made of industrial tungsten carbide based material (ISO P25/P45 type: 75% WC-15% TiC-10% Co - approximate hardness 1600 HV).

The normal load selected 10 N and the linear speed 0.6 m/s. Schematic representation of the pin-on-disc configuration together with a photograph of the tribometer used are shown in Fig. 1.
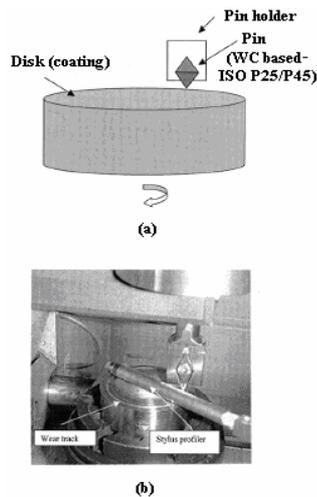

Fig 1: *(a) Schematic representation of the pin-on-disc configuration. (b) A photograph of the tribometer used.*

The coefficient of friction (μ) was deduced by the ratio F_T / F_N, (where F_T the frictional force recorded continuously during the experiment and F_N the normal applied load). The wear was evaluated by measuring with a stylus profilometer (Taylor-Hobson) the track cross-sectional area and height at ten different points on the wear track. The wear volume was calculated by multiplying the average track area (calculated by numerical integration) by the circumference of the slide circle. Tribological testing was also supported by metallography for the identification of coating microstructure alterations and wear mechanisms.

3. RESULUTS AND DISCUSSION

3.1 Surface integrity

As far as the surface integrity of the as sprayed coatings is concerned the main parameters studied were surface roughness, microhardness and microstructure in relation to arc current during deposition and the type of the substrate material.

Average values of all the surface roughness measurements are summarized in Table 2. As far as mean arithmetic surface roughness R_a is concerned, measured values are very similar; almost independent from either the pulse current or the substrate. Values of maximum surface roughness R_t decreased with increasing pulse current and moreover measured values for coatings on aluminum substrates are systematically higher than the corresponding ones for coatings on steel substrates.

Table 2. Surface roughness of Al_2O_3 ceramic coatings

Spec➜	X1	X2	X3	A1	A2	A3
$R_a(\mu m)$	4.8	4.7	4.6	4.9	4.6	4.7
$R_t(\mu m)$	42.1	34.2	34.7	38.7	36.4	36.6

For the evaluation of microstructure and the bonding integrity as well as for microhardness variation typical standardized methods were applied. A cross section of the coating/substrate system under study is presented in Fig. 2; three distinct zones, namely the upper thick Al_2O_3 coating, the intermediate bond Ni-Al layer and the steel substrate can be distinguished.
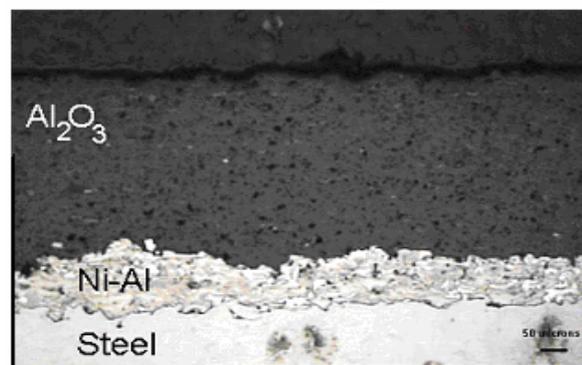

Fig. 2: *Cross section of alumina coating on steel substrate (spec. X2).*

In general, the structure of Al_2O_3 coating is characterized by the coexistence of solidified splats and both unmolten and semi-molten particles together with a certain degree of porosity. Optical metallography revealed considerable waviness at the intermediate bond/ceramic layer interface leading to variation in thickness of the former layer. Interlamellar pores, and dark particles, probably oxides, were also identified within the bond zone, mainly in the vicinity of ceramic /bond and bond/substrate interfaces. The adherence between the two coatings seems to be enhanced by the high interfacial roughness, through interlocking and anchorage mechanisms; see also [3]. Ni-Al intermediate layer/metal substrate interface is also characterized by sufficient bonding integrity caused by interlocking effect due to roughening by sand blasting. Average thickness of ceramic coatings was estimated 400-450 μm by image analysis means whilst values of 135 μm and 170 μm were measured for bond coatings on steel and aluminum substrates respectively.

The variation of microhardness below the surface of the coatings on steel and aluminum substrates is presented in Figs 3 and 4 respectively. From the plots presented in these figures it is evident that micro hardness measurements exhibit a wide fluctuation. The micro hardness of the alumina layer was estimated ranging from 793-1095 HV and from 961 to 1106 HV for coatings deposited on alumina and steal substrates respectively. Note that such dispersion in the microhardness values of the coatings is typical for APS ceramic coatings indicating microstructural hetero-geneity [9]. Average microhardness values of the coatings were found increasing with the increase of arc current during spraying; this phenomenon was more profound for coatings on aluminum substrates. Average microhardness value of intermediate bond layer was estimated 180 HV and 155 HV for coatings on aluminum and steal substrates respectively.

X-ray identification of the phases existed in the sprayed coatings was not performed. From the existing literature it is known that, for conditions used, the coating consists mainly of γ-Al_2O_3 with small amount of α-Al_2O_3, see for example [10].
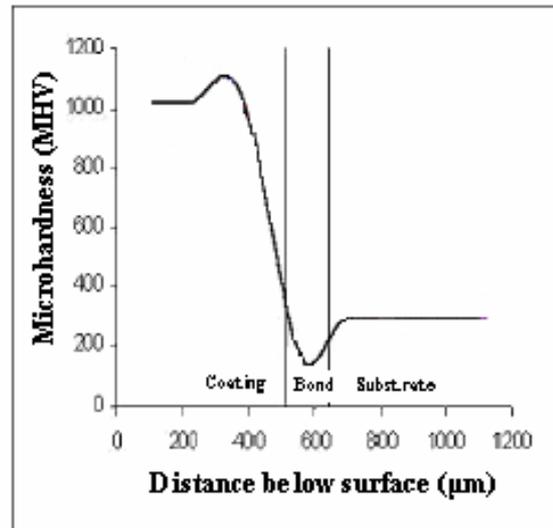

Fig. 3: *Variation of microhardness with depth below surface for a coating on steel substrate (spec. X3).*
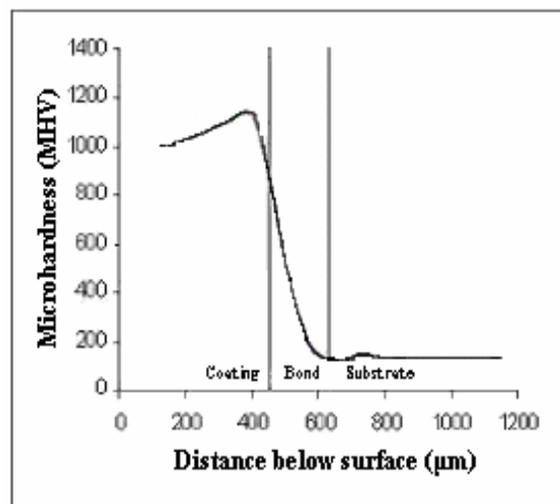

Fig. 4: *Variation of microhardness with depth below surface for a coating on steel substrate (spec. A3).*

3.2 Tribological behavior

The tribological characterization of ceramic coating included the measurement of friction coefficient and the calculation of wear rate in relation to arc current during deposition and the type of the substrate material. Predominant wear mechanism was also studied. The variation of friction coefficient with slide distance (or equivalently, time) is presented in Fig. 5. The variation presented in this plot is typical for all coatings tested. Initially a peak value is observed and then, after an intermediate oscillating stage, friction coefficient approaches

an almost constant value. The initial peak is attributed to the high surface roughness of the coating. After a number of revolutions, due to cutting of higher asperities, friction coefficient tends to be constant. Mean values of friction coefficient (μ) are summarized in Table 3.
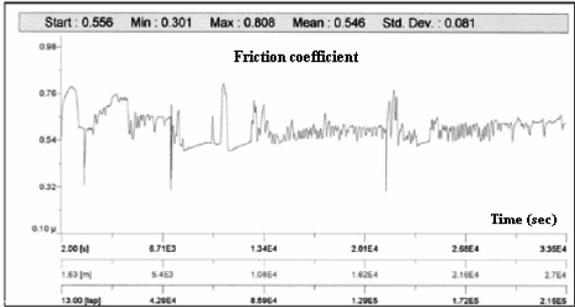

Fig 5: *Variation of friction coefficient with time (spec. X1).*

Table 3: Mean values of friction coefficient (μ).

Spec	μ	Spec	μ
X1	0.578	A1	0.565
X2	0.730	A2	0.546
X3	0.690	A3	0.600
X	0.860	A	0.650

X and A: specs of steel and aluminum respectively without coating.

From values presented in Table 3 it is concluded that friction coefficient is lower for coatings on aluminum substrate than for coatings on steel substrates. No correlations between friction coefficient and arc current were revealed.

The evolution of the wear rate of the alumina coating with slight distance is presented in Fig.6. The shape of the diagram is directly related with surface topography and possible wear mechanisms of the coating. The initial relatively high wear rate is attributed to the surface peaks of the coatings. Afterwards, the "smoothening" of coating surface and the possible wear of pin leads to an almost constant, significantly lower value. Wear rate for coatings of steel substrates was almost constant at the order of 1.3×10^{-5} and independent of arc current during deposition. For coatings on aluminum substrates dispersion of measured values was observed and mean wear rate range from 1.51×10^{-5} to 4.32×10^{-5}.
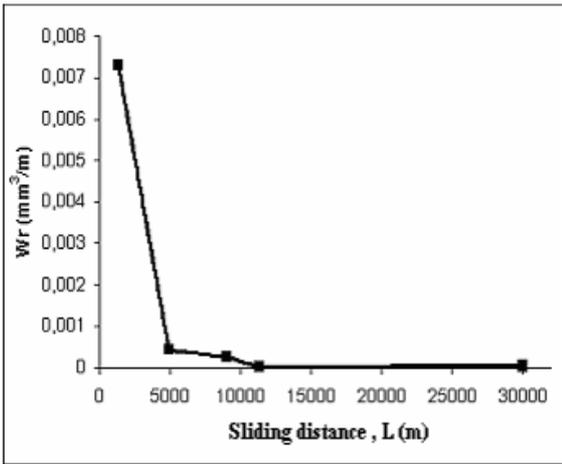

Fig. 6: *Variation of wear rate with sliding distance (spec. A3).*

For all the coatings examined, microscopic observations of the worn surfaces indicated that the wear took place mainly by abrasion and was enhanced by the exfoliation of the surface splats. The latter mechanism was also observed by other researchers see for example [9]. Abrasion should be the predominant mechanism at the initial stage of wear evolution due to shear stresses developed between the hard asperities of the two surfaces in contact.

A micrograph of worn surface of the coating is presented in Fig 7; successive parallel sliding lines can be clearly observed. This phenomenon is indicative for two different wear mechanism i.e., micro-ploughing and polishing. Moreover, observations of sections perpendicular to the wear traces showed the activation of another degradation mechanism: It was revealed that the weak interfaces between the successive lamellae failed, leading to the delamination of the coating.
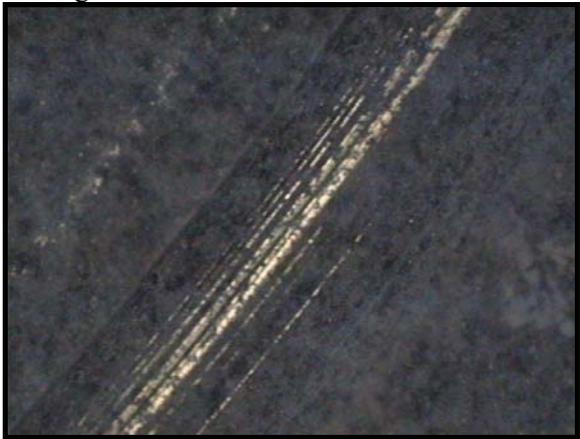

Fig 7: *Micrograph of the worn surface with sliding lines (spec X3).*

4. CONCLUSIONS

Main findings are summarized as follows:

- A typical microstructure characterized by solidified droplets and the coexistence of unmolten and semi-molten particles with a certain degree of porosity and trapped inclusions was identified in all cases.
- The microhardness of the coating increases with the increase of arc current; this phenomenon is more profound for aluminum substrates.
- Average coefficient of friction was lower for aluminum substrates than for steel ones. And was found uncorrelated with the arc current.
- Wear curves present two discrete stages. Final wear rate seems to be almost independent of the spraying parameters.
- The dominant wear mechanism is abrasion (mainly at the first stage); however, at the final stage a superimposed mechanism based on micro-ploughing, polishing and microcracking was identified under certain conditions.

REFERENCES

[1] K. Strafford and C. Subramanian, Surface engineering: an enabling technology for manufacturing industry, *J. Mater. Proc. Techn.*, 53 (1995) 393-403.

[2] R. Westergard, L.C. Erickson, N. Axen, H.M. Hawthornes and S. Hogmark, The erosion and abrasion characteristics of alumina coatings plasma sprayed under different spraying conditions, *Trib. Intl.*, 31 (1998) 271-279.

[3] D. I Pantelis, P. Psyllaki and N. Alexopoulos, Tribological behaviour of plasma-sprayed Al_2O_3 coatings under severe wear conditions, *Wear*, 237 (2000) 197-204.

[4] L. C. Erickson, H. M. Hawthorne and T. Troczynski, Correlations between micro-structural parameters, micromechanical properties and wear resistance of plasma sprayed ceramic coatings, *Wear*, 250 (2001) 569-575.

[5] B.A. Kusher and E.R. Novonski, Thermal spray coatings, friction, lubrication and wear technology, *ASM Handbook*, 18 (1992) 829-833.

[6] S.J. Bull, R. Kingswell and K.T. Scott, The sliding wear of plasma sprayed alumina, *Surf. Coat. Techn.*, 82 (1996) 218-225.

[7] L. Pawlowski, *The Science and Engineering of Thermal Spray Coatings*, 1995, Wiley, New York.

[8] A. Mamalis and N. Vaxevanidis, On the grinding of ceramic layer plasma-sprayed metal plates, (1995) SME Technical paper MR95-204.

[9] P. P. Psyllaki, M. Jeandin and D. I. Pantelis, Microstructure and wear mechanisms of thermal-sprayed alumina coatings, *Mat. Letters*, 47 (2001) 77–82.

[10] M. Uma Devi, On the nature of phases in Al_2O_3 and Al_2O_3–SiC thermal spray coatings, *Ceram. Intl.*, 30 (2004) 545–553.